Since January 2020 Elsevier has created a COVID-19 resource centre with free information in English and Mandarin on the novel coronavirus COVID-19. The COVID-19 resource centre is hosted on Elsevier Connect, the company's public news and information website.

Journal of Neuroradiology 000 (2023) 1–12

Available online at ScienceDirect www.sciencedirect.com

Elsevier Masson France EM|consulte www.em-consulte.com

Original Article

Cerebral perfusion using ASL in patients with COVID-19 and neurological manifestations: A retrospective multicenter observational study

François-Daniel Ardellier[a,c,1,*], Seyyid Baloglu[a,1], Magdalena Sokolska[b,v], Vincent Noblet[c], François Lersy[a], Olivier Collange[d], Jean-Christophe Ferré[e], Adel Maamar[f], Béatrice Carsin-Nicol[e], Julie Helms[g,h], Maleka Schenck[i], Antoine Khalil[j], Augustin Gaudemer[k], Sophie Caillard[h,l], Julien Pottecher[m], Nicolas Lefèbvre[n], Pierre-Emmanuel Zorn[o], Muriel Matthieu[o], Jean Christophe Brisset[p], Clotilde Boulay[q], Véronique Mutschler[q], Yves Hansmann[n], Paul-Michel Mertes[d], Francis Schneider[i], Samira Fafi-Kremer[r], Mickael Ohana[s], Ferhat Meziani[g,t], Nicolas Meyer[u], Tarek Yousry[v], Mathieu Anheim[q,w], François Cotton[x,y], Hans Rolf Jäger[v], Stéphane Kremer[a,c], for the SFNR-COVID group [2]

[a] *Service D'imagerie 2, Hôpital de Hautepierre, Hôpitaux Universitaires de Strasbourg, Strasbourg, France*
[b] *Department of Medical Physics and Biomedical Engineering, University College London Hospitals NHS Foundation Trust, 235 Euston Road, London NW1 2BU, United Kingdom*
[c] *Engineering science, computer science and imaging laboratory (ICube), Integrative Multimodal Imaging in Healthcare, UMR 7357, University of Strasbourg-CNRS, Strasbourg, France*
[d] *Service d'Anesthésie-Réanimation, Nouvel Hôpital Civil, Hôpitaux universitaires de Strasbourg, Strasbourg, France*
[e] *Department of Neuroradiology, CHU Rennes, Rennes, France*
[f] *Medical Intensive Care Unit, CHU Rennes, Rennes, France*
[g] *Service de Médecine Intensive Réanimation, Nouvel Hôpital Civil, Hôpitaux Universitaires de Strasbourg, Strasbourg, France*
[h] *Immuno-Rhumatologie Moléculaire, INSERM UMR S1109, LabEx TRANSPLANTEX, Centre de Recherche d'Immunologie et d'Hématologie, Faculté de Médecine, Fédération Hospitalo-Universitaire (FHU) OMICARE, Fédération de Médecine Translationnelle de Strasbourg (FMTS), Université de Strasbourg (UNISTRA), Strasbourg, France*
[i] *Service de Médecine Intensive Réanimation, Hôpitaux universitaires de Strasbourg, Hautepierre, Strasbourg, France*
[j] *Department of Radiology, Assistance Publique–Hôpitaux de Paris (APHP), Denis Diderot University and Medical School, Bichat University Hospital, Paris, France*
[k] *Neuroradiology Unit, Department of Radiology, Assistance Publique-Hôpitaux de Paris (APHP), Bichat University Hospital, Paris, France*
[l] *Nephrology and Transplantation department, Hôpitaux Universitaires de Strasbourg. Inserm UMR S1109, LabEx Transplantex, Fédération de Médecine Translationnelle de Strasbourg (FMTS), Université de Strasbourg, Strasbourg, France*
[m] *Hôpital de Hautepierre, Service d'Anesthésie, Réanimation & Médecine Péri-Opératoire - Université de Strasbourg, Faculté de Médecine, FMTS, EA3072, Hôpitaux Universitaires de Strasbourg, Strasbourg, France*
[n] *Service de Maladies Infectieuses, NHC, CHU de Strasbourg, Strasbourg, France*
[o] *Hôpitaux Universitaires de Strasbourg, UCIEC, Pôle d'Imagerie, Strasbourg, France*
[p] *Brisset-Li Consulting, Valbonne-Sophia-Antipolis, France*
[q] *Service de Neurologie, Hôpitaux Universitaires de Strasbourg, Strasbourg, France*
[r] *Laboratoire de Virologie Médicale, Hôpitaux Universitaires de Strasbourg, Strasbourg, France*
[s] *Radiology Department, Nouvel Hôpital Civil, Strasbourg University Hospital, Strasbourg, France*
[t] *UMR 1260, Regenerative Nanomedicine (RNM), FMTS, INSERM (French National Institute of Health and Medical Research), Strasbourg, France*
[u] *Service de Santé Publique, GMRC, CHU de Strasbourg, Strasbourg F-67091 , France*
[v] *Neuroradiological Academic Unit, Department of Brain Repair and Rehabilitation, UCL Queen Square Institute of Neurology, Queen Square, London WC1N 3BG, United Kingdom*
[w] *INSERM-U964/CNRS-UMR7104/Université de Strasbourg, Institut de Génétique et de Biologie Moléculaire et Cellulaire (IGBMC), Illkirch, France*
[x] *MRI center, Centre Hospitalier Lyon Sud, Hospices Civils de Lyon, Lyon, France*
[y] *CREATIS-LRMN, CNRS/UMR/5220-INSERM U630, Université Lyon 1, Villeurbanne, France*

Abbreviations: COVID-19, coronavirus disease 2019; SARS-CoV-2, severe acute respiratory syndrome coronavirus 2; ICU, intensive-care unit; ASL, arterial spin labeling; CBF, cerebral blood flow; RT-PCR, reverse transcriptase-polymerase chain reaction; EEG, electroencephalogram; PaO_2, partial pressure of arterial oxygen; FiO_2, fraction of inspired oxygen

* Corresponding author at: Service D'imagerie 2, Hôpital de Hautepierre, Hôpitaux Universitaires de Strasbourg, Strasbourg, France.
E-mail address: francois-daniel.ardellier@chru-strasbourg.fr (F.-D. Ardellier).

[1] These authors contributed equally to this work.

[2] SFNR-COVID group:
Toulouse University Hospital (Toulouse) : Fabrice Bonneville, Gilles Adam, Guillaume Martin-Blondel, Jérémie Pariente, Thomas Geeraerts ; Louis Pasteur Hospital (Colmar) : Hélène Oesterlé, Federico Bolognini, Julien Messie ; Sainte-Anne Hospital (Paris) : Ghazi Hmeydia, Joseph Benzakoun, Catherine Oppenheim ; Amiens University Hospital (Amiens) : Jean-Marc Constans, Serge Metanbou, Adrien Heintz ; Henri-Mondor University Hospital (Créteil) : Blanche Bapst, Imen Megdiche ; CHIC Unisanté (Forbach) : Lavinia Jager, Patrick Nesser, Yannick Talla Mba ; Bordeaux University Hospital (Bordeaux) : Thomas Tourdias, Juliette Coutureau ; Emile Muller Hospital (Mulhouse) : Céline Hemmert, Philippe Feuerstein, Nathan Sebag ; Hospital of Haguenau (Haguenau) : Sophie Carre, Manel Alleg, Claire Lecocq ; Nancy University Hospital (Nancy) : Emmanuel Schmitt, René Anxionnat, François Zhu ; Limoges University Hospital (Limoges) : Géraud Forestier, Aymeric Rouchaud ; Dijon University Hospital (Dijon) : Pierre-Olivier Comby, Frederic Ricolfi, Pierre Thouant ; Grenoble Alpes University Hospital (Grenoble) : Sylvie Grand, Alexandre Krainik ; Antony Private Hospital (Antony) : Isaure de Beaurepaire, Grégoire Bornet ; Hospices Civils de Lyon (Lyon) : Audrey Lacalm, Patrick Miailhes, Julie Pique ; Saint-Etienne University Hospital (Saint-Etienne) : Claire Boutet, Xavier Fabre ; Clermont-Ferrand University Hospital (Clermont-Ferrand) : Béatrice Claise, Sonia Mirafzal, Laure Calvet ; French Neuroradiological Society (SFNR) board : Hubert Desal, Jérome Berge, Grégoire Boulouis, Apolline Kazemi, Nadya Pyatigorskaya, Augustin Lecler, Suzana Saleme, Myriam Edjlali-Goujon, Basile Kerleroux, Jean-Christophe Brisset ; UCIEC : Samir Chenaf

https://doi.org/10.1016/j.neurad.2023.01.005

Please cite this article as: F.-D. Ardellier, S. Baloglu, M. Sokolska et al., Cerebral perfusion using ASL in patients with COVID-19 and neurological manifestations: A retrospective multicenter observational study, Journal of Neuroradiology (2023), https://doi.org/10.1016/j.neurad.2023.01.005

ARTICLE INFO

Article History:
Available online xxx

Keywords:
COVID-19
Neuroimaging
Magnetic resonance imaging
Cerebrovascular circulation
Multicenter study

ABSTRACT

Background and purpose: Cerebral hypoperfusion has been reported in patients with COVID-19 and neurological manifestations in small cohorts. We aimed to systematically assess changes in cerebral perfusion in a cohort of 59 of these patients, with or without abnormalities on morphological MRI sequences.
Methods: Patients with biologically-confirmed COVID-19 and neurological manifestations undergoing a brain MRI with technically adequate arterial spin labeling (ASL) perfusion were included in this retrospective multicenter study. ASL maps were jointly reviewed by two readers blinded to clinical data. They assessed abnormal perfusion in four regions of interest in each brain hemisphere: frontal lobe, parietal lobe, posterior temporal lobe, and temporal pole extended to the amygdalo-hippocampal complex.
Results: Fifty-nine patients (44 men (75%), mean age 61.2 years) were included. Most patients had a severe COVID-19, 57 (97%) needed oxygen therapy and 43 (73%) were hospitalized in intensive care unit at the time of MRI. Morphological brain MRI was abnormal in 44 (75%) patients. ASL perfusion was abnormal in 53 (90%) patients, and particularly in all patients with normal morphological MRI. Hypoperfusion occurred in 48 (81%) patients, mostly in temporal poles (52 (44%)) and frontal lobes (40 (34%)). Hyperperfusion occurred in 9 (15%) patients and was closely associated with post-contrast FLAIR leptomeningeal enhancement (100% [66.4%-100%] of hyperperfusion with enhancement versus 28.6% [16.6%-43.2%] without, $p = 0.002$). Studied clinical parameters (especially sedation) and other morphological MRI anomalies had no significant impact on perfusion anomalies.
Conclusion: Brain ASL perfusion showed hypoperfusion in more than 80% of patients with severe COVID-19, with or without visible lesion on conventional MRI abnormalities.

The current outbreak of severe acute respiratory syndrome coronavirus 2 (SARS-CoV-2) is a major health issue, with more than 615 million cases of coronavirus disease 2019 (COVID-19) worldwide as of September 26th, 2022,[1] causing 6.5 million deaths. In France, in 2020, 46,000 patients were admitted in intensive care unit (ICU) for COVID-19, corresponding to almost one tenth of the hospitalization days in these units. An operational retrospective definition of severe COVID-19 is the need for hospitalization (in ICU or in conventional ward) and oxygen therapy, as such care is required for patients with respiratory signs usually used to define severe illness (marked tachypnea and hypoxia).[2] In such hospitalized patients, neurological manifestations were initially seldom described, probably masked by the severity of the respiratory and systemic symptoms, but are increasingly reported.[3–5] About half of these patients with neurological manifestations have pathological findings on "classical" morphological magnetic resonance imaging (MRI).[6,7]

Arterial spin labeling (ASL) is a versatile non-contrast MRI sequence routinely used to assess cerebral perfusion, which quantitatively measures cerebral blood flow (CBF).[8] Among many other applications, it has been used to unveil cerebral perfusion alterations in central nervous system infections[9] or in autoimmune encephalitis.[10] Cerebral perfusion impairment has been seldomly reported in patients with COVID-19.[4,7] Using ASL perfusion sequence, this study aimed to systematically assess cerebral perfusion changes in a multicentric retrospective cohort of patients with severe COVID-19 and neurological symptoms.

Material and methods

This retrospective national multicenter observational study was approved by an ethical committee and was conducted in accordance with the 1964 Helsinki Declaration and its later amendments. Given its retrospective and observational design, the requirement for patients' written informed consent was waived.

Consecutive patients with COVID-19 infection and neurologic manifestations requiring brain MRI were included from February 14th, 2020, to May 1st, 2020, in 17 French centers, including 11 university hospitals and 6 general hospitals. Inclusion criteria were: (i) diagnosis of COVID-19 validated with a detection of SARS-CoV-2 by reverse transcriptase-polymerase chain reaction (RT-PCR) assays on the nasopharyngeal, throat or lower respiratory tract swabs; (ii) neurologic manifestations; (iii) brain MRI with ASL perfusion. ASL perfusion was preferred for two reasons. First, it allows quantitative measurement of CBF with readily available maps without the variability induced by manual post-processing of dynamic susceptibility contrast perfusion. Second, it is less sensitive to susceptibility artifacts as hemorrhagic lesions are frequent in patients with COVID-19.[11] Exclusion criteria were: (i) patients with non-contributory data regarding ASL sequence (artifacts); (ii) perfusion anomalies related to a chronic lesion (i.e. unrelated to the current event, like porencephalic cavities or surgical sequalae), (iii) acute perfusion anomalies related to an intracranial large vessel occlusion or significant stenosis. A brief description of cerebral perfusion data of 11 patients has previously been published.[4] These patients are still included in the present study where their data were more extensively analyzed.

Fourteen healthy volunteers matched for age without psychiatric or neurological history (except for migraine) were enrolled after written informed consent was obtained and underwent 3D pseudo-continuous (the most common method of spin-labeling) ASL perfusion at one of the participating centers equipped with a 3T scanner.

Clinical and laboratory data (SARS-CoV-2 RT-PCR, CSF sample analysis) were extracted from the patients' electronic medical records in the Hospital Information System. Clinical data included medical history (neurological history, history of hematological malignancies or autoimmune diseases), symptoms and signs (psychomotor agitation, ageusia, anosmia, headaches, seizures, confusion, clinical signs of corticospinal tract involvement, disturbance of consciousness, acute respiratory distress syndrome), chest CT findings, oxygen therapy and sedation. Symptoms or oxygen therapy were considered present if they occurred at any time before MRI. Data on oxygen therapy and anesthetic drugs used at the time of MRI were not available. In accordance with Berlin criteria, acute respiratory distress syndrome was defined as a ratio between partial pressure of arterial oxygen (PaO_2) and fraction of inspired oxygen (FiO_2) below 300 mmHg. Death from any cause was registered up to 30 days after MRI.

Alike ASL perfusion, electroencephalogram (EEG) provides functional information on the brain. This might help understand perfusion abnormalities. Hence, all available EEGs were reviewed by one expert neurologist and classified into five groups (normal, under sedation, nonspecific, encephalopathy or seizures) for comparison with brain perfusion.

Qualitative analysis

Imaging studies were conducted either on 1.5 Tesla or 3 Tesla MRI (90% were performed at 3T). All MRI were performed in supine position. The multicenter nature of the study and the various clinical set-ups did not allow standardization of sequences. All centers used standard dose (0,1 mmol/kg) of macrocyclic gadolinium-based contrast agent. Most post-contrast FLAIR were three-dimensional sequences, with repetition times, echo times and inversion times respectively ranging from 4800 ms to 6000 ms, 290 ms to 393 ms and 1650 ms to 1842 ms, and slice thickness usually less or equal 1 mm. All ASL perfusion used pseudo-continuous tagging, with post-labeling delay ranging from 1525 ms to 2025 ms. All centers but one (12 patients) used 3D readouts for ASL. CBF maps were automatically created by the MRI scanners at the time of acquisition for all patients but two that provided only perfusion weighted images (Siemens MRI scanner). Imaging studies were jointly reviewed by two neuroradiologists (F-D.A. and S.B., with eight and nine years of experience, respectively), with the help of a third one in case of discordance (S.K., with 20 years of experience). Raters were blinded to clinical data except for the SARS-CoV-2 infection to prevent potential bias in MRI review (in case a link between MRI abnormalities and clinical data had emerged during review and induced changes in MRI evaluation based on clinical data). Based on preliminary observations,[4] perfusion images (CBF maps or perfusion weighted images) were analyzed in 4 regions in each brain hemisphere: frontal lobe, parietal lobe, posterior temporal lobe, and temporal pole extended to the amygdalo-hippocampal complex. Occipital lobes were excluded from the regional analysis due to high perfusion variability along with visual attention which was not retrospectively assessable. Brainstem and cerebellum were excluded because they were only partially included in most ASL sequences. Examples of altered perfusion are provided in Fig. 2. All perfusion maps were displayed as color maps using the Acute Stroke Imaging Standardization Group (ASIST) lookup table. Using a clinical set-up, cerebral perfusion was visually rated in each region as hypoperfusion, normal perfusion or hyperperfusion. This qualitative analysis was not strictly standardized, and reviewers were instructed to evaluated CBF maps as they would have in a routine reading to approximate “real-life”. For further analysis, perfusion was considered abnormal (either hyperperfusion or hypoperfusion) at the patient level if perfusion was abnormal in at least one brain region.

Morphological analysis followed the eight patterns described by Kremer et al.[11] These patterns are descriptive, based on the spatial distribution of FLAIR and/or diffusion abnormalities and the presence or absence of hemorrhagic lesions. In addition, leptomeningeal enhancement (on post-contrast FLAIR sequence), ischemic stroke and miscellaneous acute findings were assessed. An example of leptomeningeal enhancement is provided in Fig. 3.

Quantitative subgroup analysis

For the sake of data homogeneity, we conducted a quantitative analysis of perfusion data by considering a restricted subgroup of 11 patients and 14 healthy volunteers that all underwent a 3D pseudo-continuous ASL perfusion on the same 3T GE Signa HD scanner (voxels: 1.875 × 1.875 × 4 mm, repetition time: 4599 ms, echo time: 9.8 ms, post-labeling delay: 1525 ms). CBF maps were generated using MRI manufacturer software. To allow voxel-based analysis, all these images were affinely registered in the MNI-space using the ANTs library (http://stnava.github.io/ANTs/). Intensity was then normalized by the average whole brain CBF and smoothed with an 8 mm FWHM gaussian kernel. Voxel-based group comparison was conducted using Statistical Parametric Mapping (SPM, https://www.fil.ion.ucl.ac.uk/spm/) while considering age and sedation as covariate.

Statistical analysis

Statistical analyses were performed with R 4.0.3[12] (R Foundation for Statistical Computing, Vienna, Austria). Continuous data are reported as mean, median and range, discrete data as frequency and proportion. Categorical data were compared using Fischer exact test. Quantitative data were compared using Student’s *t*-test for normally distributed variables and Wilcoxon rank-sum test otherwise. Uncorrected 95% confidence intervals (bootstrapped for medians) are reported. A false discovery rate of 5% (with Benjamini-Hochberg procedure) was used to correct p-values for multiple testing (i.e. a corrected p-value lower than 0.05 was considered significant).

Quantitative voxel-based statistical analysis of CBF maps were conducted using the general linear model to objectify differences between patients and control while considering age and sedation as covariates. Thresholded p-value maps ($p < 0.001$, uncorrected) were superimposed on the T1 weighted MRI of MNI brain template.

Results

Among the 192 screened patients (Fig. 1) with a brain MRI, 83 (43%) had an ASL perfusion sequence. Twenty patients were excluded: (i) 17 patients with technically inadequate ASL perfusion (movements artifacts, aliasing artifacts, or severe arterial transit time artifact); (ii) 1 patient with left hemisphere apparent hypoperfusion with unknown cervical artery status; (iii) 1 patient with proximal right middle cerebral artery occlusion; (iv) 4 patients with clinically diagnosed COVID-19 but without a positive RT-PCR for SARS-CoV-2.

Ultimately, 59 patients from 3 university hospital were analyzed. Most patients suffered from severe COVID-19: 57 (97%) needed oxygen therapy during hospitalization and 43 (73%) were hospitalized in ICU at the time of MRI. 49 (83%) had an intracranial MR angiography, none of them with significant intracranial arterial stenosis. Other demographic and clinical data are shown in Table 1.

Qualitative analysis

Morphological brain MRI was abnormal in 44 patients (75%), leptomeningeal enhancement being the most frequently encountered feature (see Table 2). Fifty-three (90%) patients had an abnormal cerebral perfusion, without significant difference across hospitals ($p = 0.85$) or across variations of ASL sequence parameters (post-labeling delay ($p > 0.999$) and type of readout ($p = 0.73$)). All patients with a normal morphological MRI had abnormal cerebral perfusion, whereas 6 (14%) patients with abnormal morphological MRI had normal perfusion. Hypoperfusion was more frequently encountered than hyperperfusion (48 (81%) versus 9 (15%), $p < 0.001$). Leptomeningeal enhancement was positively associated with hyperperfusion: all patients (100% [66.4–100%]) with hyperperfusion had leptomeningeal enhancement whereas 28.6% [16.6–43.2%] patients without hyperperfusion had leptomeningeal enhancement, $p = 0.002$. Among 14 patients with leptomeningeal enhancement but without hyperperfusion, 11 (79%) had hypoperfusion and 3 (21%) had no perfusion abnormality. Cerebral perfusion was not significantly different for patients in ICU at the time of MRI compared to patients admitted in conventional wards (91.0% [58.8–99.8%] of patients without hypoperfusion being in ICU versus 68.8% [53.8–81.4%] of patients with hypoperfusion, $p = 0.92$, and 68% [53.4–80.4%] of patients without hyperperfusion being in ICU versus 100% [66.4–100%] of patients with hyperperfusion, $p = 0.77$). Perfusion was also not significantly different for sedated patients compared to awake ones (36.4% [11.0–69.2%] of patients without hypoperfusion being sedated versus 43.8% [29.4–58.8%] of patients with hypoperfusion, $p > 0.999$, and 38% [24.6–52.8%] of patients without hyperperfusion being sedated versus 66.6% [30–92.6%] of patients with hyperperfusion, $p = 0.85$). Patients with abnormal cerebral perfusion tended to have a non-

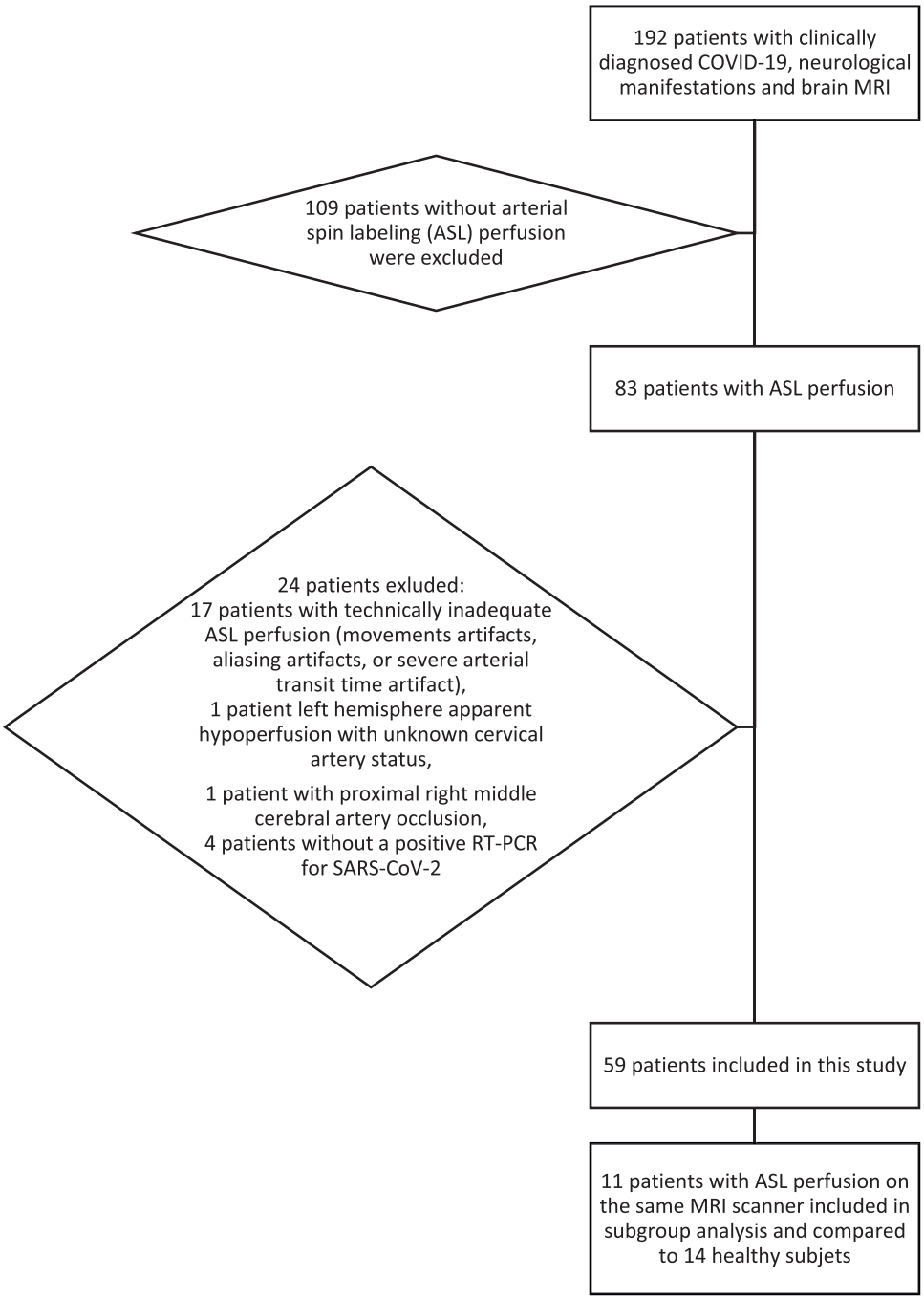

Fig. 1. Flowchart of patient inclusion.

significant shorter delay between symptoms onset and MRI (mean delay 25.3 [22.5–28] days versus 32.3 [28–36.7] days, $p = 0.12$). There was no significant difference for the delay between hospitalization and MRI (median delay 7 [5–7] days versus 6.5 [2–9.5] days, $p > 0.999$). The other clinical (either comorbidities or symptoms), biological, and morphological imaging recorded parameters were not significantly associated with cerebral perfusion changes (see Tables 3 and 4). Patients with extensive white matter microhemorrhage had a longer delay between symptoms onset and MRI (mean delay 34.6 [30.9–38.4] days versus 23.9 [21.2–26.7] days, $p = 0.001$).

Regional qualitative perfusion did not differ significantly across cerebral hemispheres ($p = 0.29$) but varied significantly across the four analyzed brain regions ($p < 0.001$), with abnormal perfusion ranging from 22.9% to 49.6% of the cases (Table 5). Temporal pole and frontal lobe were the most frequent sites of hypoperfusion (in respectively 52 (44%) and 40 (34%) of the analyzed brain hemispheres), whereas hyperperfusion occurred most frequently in parietal and temporal lobe (in respectively 18 (15%) and 16 (14%) of the analyzed brain hemispheres). Leptomeningeal enhancement was associated with hyperperfusion in temporal, parietal and frontal lobe (leptomeningeal enhancement being present in 28.6% [16.6–43.2%] of patients without hyperperfusion in temporal and parietal lobe, and 30% [17.8–44.6%] in frontal lobe, versus 100% [66.4–100%] of patients with hyperperfusion in temporal and parietal lobe, and 100% [63–100%] in frontal lobe, $p = 0.006$, $p = 0.006$ and $p = 0.01$, respectively). There was no other significant association between regional hypoperfusion or hyperperfusion and clinical, biological or morphological MRI findings.

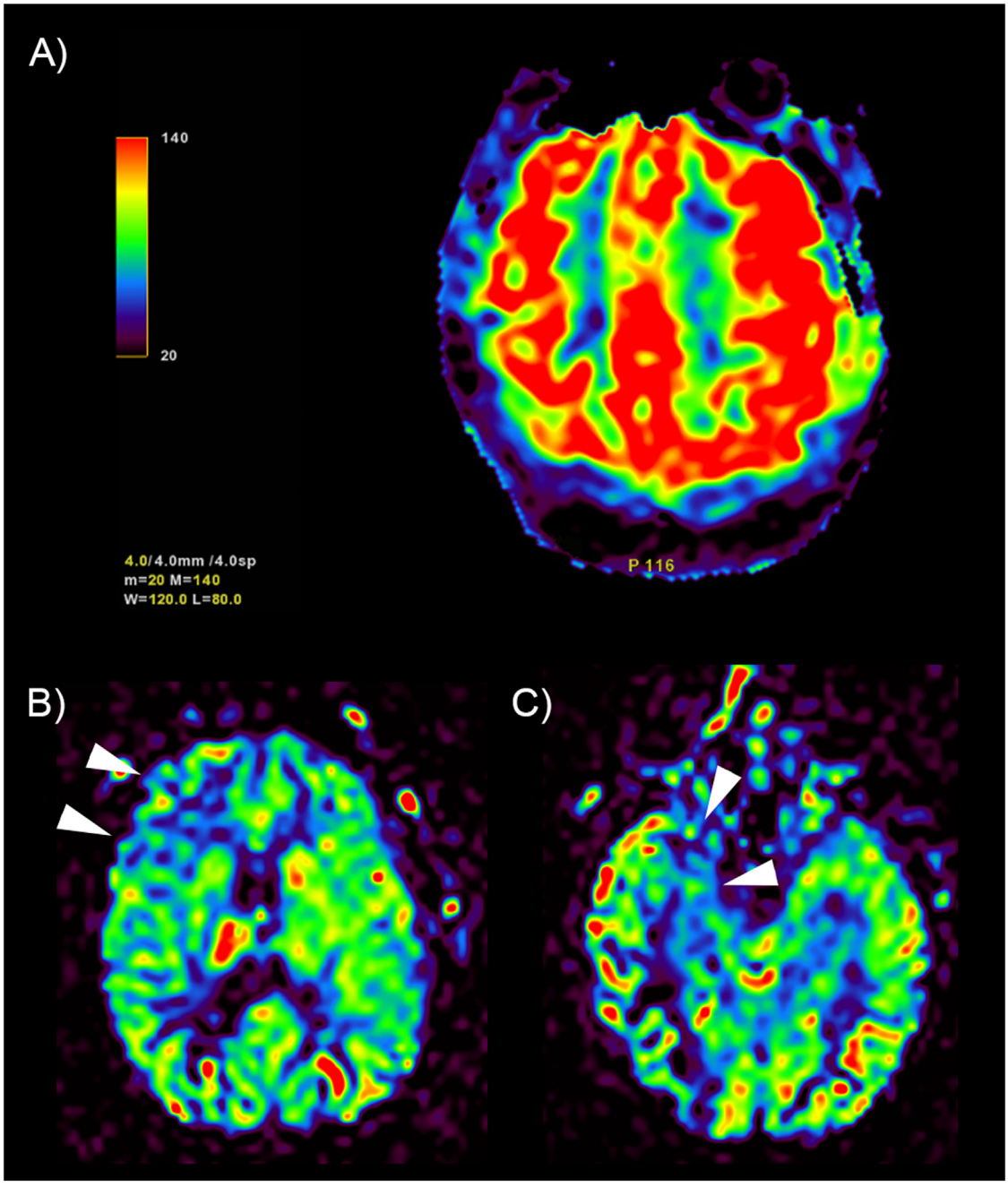

Fig. 2. Examples of perfusion anomalies qualitatively assessed on cerebral blood flow maps. (A) bilateral frontoparietal hyperperfusion (color scale on the left in mL/100 mg/min). Arrowheads: hypoperfusion in right frontal (B) and temporopolar (C) regions in the same patient.

Subgroup analysis

Fourteen controls (5 men (36%), mean age 52.9 years, median age 52 years, range [48−61]) were compared to a subgroup of 11 patients (7 men (64%), mean age 62 years, median age 66 years, range [20 −81]). Controls were significantly younger than patients (p = 0.006). No hyperperfusion was seen in controls (0 (0%) versus 8 (73%), p = 0.0008). There was more hypoperfusion in patients than in the control group (respectively 1 (7%) and 7 (64%) in controls and patients, p = 0.009).

Mean perfusion maps (Fig. 4) show a large fronto-temporal pattern of hypoperfusion in patients with COVID-19. Quantitative analysis corrected for age and sedation retains significant bilateral posterior fronto-opercular, insular and temporopolar clusters of hypoperfusion (Fig. 5). There were also bilateral clusters of hyperperfusion along precentral and frontal superior gyrus, and smaller parietal clusters. Significant hyperperfusion was also seen at the superior part of the cerebellum.

Discussion

In this large cohort of patients with severe COVID-19, we found frequent cerebral perfusion alteration. Hypoperfusion occurred in a bilateral frontal and temporo-polar pattern. Hyperperfusion was less frequent, affecting bilateral parieto-temporal regions, with a strong association with leptomeningeal enhancement. Smaller hyperperfusion clusters were detected in subgroup analysis near motor and premotor cortices.

In the qualitative analysis, the absence of systematic measurements of CBF could have led to errors, with areas of normal perfusion

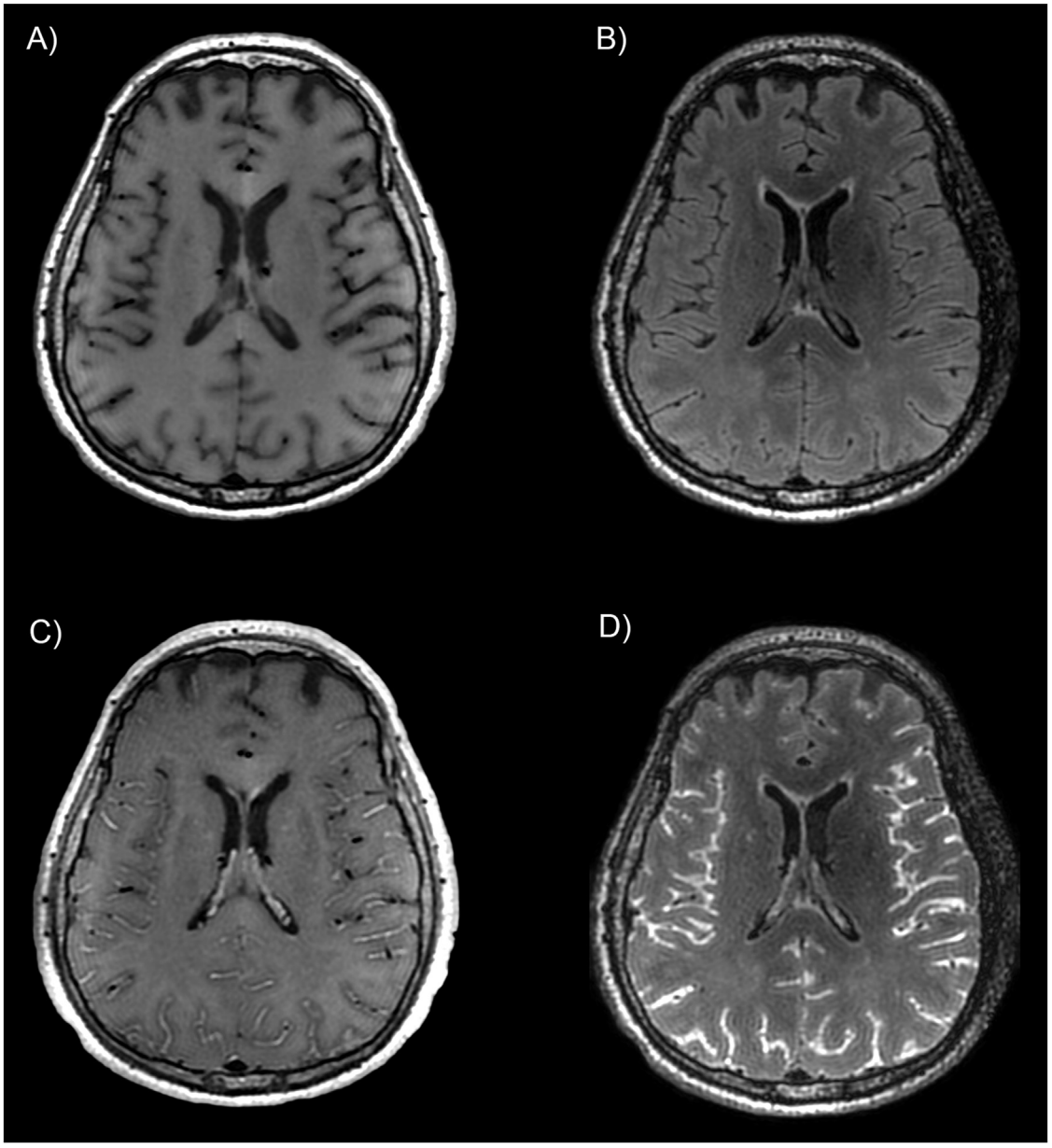

Fig. 3. Example of leptomeningeal enhancement in a patient with COVID-19. Spin-echo T1-weighted and FLAIR sequences before (A and B) and after (C and D) injection of gadolinium-based contrast agent, showing a diffuse leptomeningeal enhancement after injection. In this study, post-contrast FLAIR was the reference sequence used to assess leptomeningeal enhancement.

near areas of hyperperfusion being wrongly identified as hypoperfusion near normal perfusion, or vice versa. However, the pattern of brain hypoperfusion in patients with COVID-19 visible on mean perfusion maps and quantitative analysis matched the pattern of the qualitative analysis. This supports the results of the qualitative analysis and the existence of (non-mislabeled) brain hypoperfusion in patients with severe COVID-19 detectable not only in group analysis but also in individual patients in a clinical set-up.

Could perfusion abnormalities be related to COVID-19?

Various cerebral perfusion abnormalities have previously been described in encephalitis, whether of auto-immune or viral origin. Hypoperfusion and hyperperfusion can either develop simultaneously in different brain locations or arise sequentially in the same location. In *Herpes simplex* virus encephalitis, there is an initial phase of temporal hyperperfusion, followed by a subsequent hypoperfusion.[9,13] A similar evolution pattern is described in Japanese encephalitis, with thalamus hyperperfusion in the acute phase, followed by a fronto-parietal hypoperfusion in the subacute phase and thalamus hypoperfusion in the chronic phase.[14] In tick-born encephalitis, hyperperfusion can be detected in thalamus.[15] Both hypoperfusion and hyperperfusion have been described in progressive multifocal leukoencephalopathy due to John Cunningham virus.[9,16] Human immunodeficiency virus encephalopathy is associated with a reduced CBF in frontal and parietal lobes, and in lenticular nuclei.[17] Occipito-parietal and mesial temporal hypoperfusion have been reported in N-methyl-D-aspartate receptor (NMDAR) encephalitis with normal conventional MRI.[18] The similarities in patterns of perfusion abnormalities between these encephalitis and the ones reported in this study suggest that COVID-19 induces these abnormalities. In COVID-19, the trend observed between short symptoms-

Table 1
Demographic and clinical characteristics of the patients.

	Patients (n = 59)
Sex *(Men / Woman)*	44 (74.6%) / 15 (25.4%)
Age (years) *(Mean / median / range)*	61.2 / 63 / 20–81
Time from symptoms onset to first hospital admission (days) *(Mean / median / range)*	8.4 / 7 / 2–31
Time from symptoms onset to brain MRI (days) *(Mean / median / range)*	26 / 27 / 5–47
Chest CT findings suggestive of COVID-19	
Positive	50 (84.7%)
Negative	4 (6.8%)
Not realized	5 (8.5%)
RT-PCR SARS-CoV-2 on upper or lower respiratory tract swabs	59 (100%)
RT-PCR SARS-CoV-2 on CSF	
Positive	3 (5.1%)
Negative	33 (55.9%)
Not realized	23 (39%)
Oxygen therapy at any time during hospitalization	57 (96.6%)
Acute respiratory distress syndrome	51 (86.4%)
Hospitalized in intensive care unit at time of MRI	43 (72.9%)
Sedation during MRI or up to 24 h before MRI	25 (42.4%)
Death up to 30 days after MRI	6 (10.2%)
Medical history	
History of stroke	7 (11.9%)
History of seizures	3 (5.1%)
Other neurological history	8 (13.6%)
History of autoimmune diseases	4 (6.8%)
History of hematological malignancies	3 (5.1%)
Symptoms at any time before MRI	
Headaches	12 (20.3%)
Seizures	2 (3.4%)
Anosmia	7 (11.9%)
Ageusia	7 (11.9%)
Clinical signs of corticospinal tract involvement	16 (27.1%)
Disturbance of consciousness	40 (67.8%)
Confusion	25 (42.4%)
Agitation	21 (35.6%)
Electroencephalogram	
Normal	4 (6.8%)
Under sedation	9 (15.3%)
Nonspecific	10 (16.9%)
Encephalopathy	7 (11.9%)
Seizures	0 (0%)
Not realized	29 (49.2%)

Table 2
Neuroimaging findings.

	Patients (n = 59)
Number of enhanced brain MRI	58 (98.3%)
Number of abnormal morphological brain MRI*	44 (74.6%)
Ischemic stroke	6 (10.2%)
Leptomeningeal enhancement†	23 (39%)†
Mesial temporal lobe diffusion/FLAIR hyperintensity	13 (22%)
Non-confluent multifocal white matter diffusion/FLAIR hyperintense lesions with hemorrhage and variable enhancement	7 (11.9%)
Extensive and isolated white matter microhemorrhages	13 (22%)
Extensive and confluent supratentorial white matter FLAIR hyperintensities	1 (1.7%)
Diffusion/FLAIR hyperintense ovoid lesion in the corpus callosum	0 (0%)
Non-confluent multifocal white matter diffusion/FLAIR hyperintense lesions with variable enhancement	4 (6.8%)
Acute necrotizing encephalopathy	0 (0%)
Diffusion/FLAIR hyperintense lesions involving both middle cerebellar peduncles	1 (1.7%)
Other	2 (3.4%)
Number of abnormal ASL perfusion*	53 (89.8%)
Hypoperfusion	48 (81.4%)
Hyperperfusion	9 (15.3%)

* Patient can have more than one MRI anomaly.
† assessable only in 58 patients with enhanced MRI.

Table 3
Relationship between cerebral hypoperfusion and clinical, biological and morphological parameters.

	No hypoperfusion† (*N* = 11)	Hypoperfusion† (*N* = 48)	Corrected p-value†
Men	7 (63.6% [30.8–89%])	37 (77% [62.6–88%])	>0.999
Oxygen therapy	11 (100% [71.6–100%])	46 (95.8% [85.8–99.4%])	>0.999
Acute respiratory distress syndrome	11 (100% [71.6–100%])	40 (83.4% [69.8–92.6%])	0.962
Hospitalized in intensive care unit at time of MRI	10 (91% [58.8–99.8%])	33 (68.8% [53.8–81.4%])	0.919
Sedation during MRI or up to 24 h **before MRI**	4 (36.4% [11–69.2%])	21 (43.8% [29.4–58.8%])	>0.999
Death up to 30 days after MRI	0 (0% [0–28.4%])	6 (12.4% [4.8–25.2%])	>0.999
Chest CT findings suggestive of COVID-19‡	8 (100% [63–100%])	42 (91.4% [79.2–97.6%])	>0.999
Medical history			
History of stroke	2 (18.2% [2.2–51.8%])	5 (10.4% [3.4–22.6%])	>0.999
History of seizures	0 (0% [0–28.4%])	3 (6.2% [1.4–17.2%])	>0.999
Other neurological history	0 (0% [0–28.4%])	8 (16.6% [7.4–30.2%])	0.962
History of hematological malignancies	0 (0% [0–28.4%])	3 (6.2% [1.4–17.2%])	>0.999
History of autoimmune diseases	1 (9% [0.2–41.2%])	3 (6.2% [1.4–17.2%])	>0.999
Symptoms			
Agitation	6 (54.6% [23.4–83.2%])	15 (31.2% [18.6–46.2%])	0.852
Ageusia	1 (9% [0.2–41.2%])	6 (12.4% [4.8–25.2%])	>0.999
Anosmia	1 (9% [0.2–41.2%])	6 (12.4% [4.8–25.2%])	>0.999
Headaches	2 (18.2% [2.2–51.8%])	10 (20.8% [10.4–35%])	>0.999
Seizures	1 (9% [0.2–41.2%])	1 (2% [0–11%])	0.962
Confusion	6 (54.6% [23.4–83.2%])	19 (39.6% [25.8–54.8%])	>0.999
Clinical signs of corticospinal tract involvement	2 (18.2% [2.2–51.8%])	14 (29.2% [17–44%])	>0.999
Disturbance of consciousness	9 (81.8% [48.2–97.8%])	31 (64.6% [49.4–77.8%])	>0.999
Electroencephalogram‡			
Normal	1 (14.2% [0.4–57.8%])	3 (13% [2.8–33.6%])	>0.999
Under sedation	1 (14.2% [0.4–57.8%])	8 (34.8% [16.4–57.2%])	>0.999
Nonspecific	4 (57.2% [18.4–90.2%])	6 (26% [10.2–48.4%])	0.852
Encephalopathy	1 (14.2% [0.4–57.8%])	6 (26% [10.2–48.4%])	>0.999
Morphological MRI findings			
Ischemic stroke	2 (18.2% [2.2–51.8%])	4 (8.4% [2.4–20%])	0.962
Leptomeningeal enhancement‡	8 (72.8% [39–94%])	15 (32% [19–47.2%])	0.292
Mesial temporal lobe diffusion/FLAIR hyperintensity	3 (27.2% [6–61%])	10 (20.8% [10.4–35%])	>0.999
Non-confluent multifocal white matter diffusion/FLAIR hyperintense lesions with hemorrhage and variable enhancement	1 (9% [0.2–41.2%])	6 (12.4% [4.8–25.2%])	>0.999
Extensive and isolated white matter microhemorrhages	5 (45.4% [16.8–76.6%])	8 (16.6% [7.4–30.2%])	0.504
Extensive and confluent supratentorial white matter FLAIR hyperintensities	1 (9% [0.2–41.2%])	0 (0% [0–7.4%])	0.852
Non-confluent multifocal white matter diffusion/FLAIR hyperintense lesions with variable enhancement	0 (0% [0–28.4%])	4 (8.4% [2.4–20%])	>0.999
Diffusion/FLAIR hyperintense lesions involving both middle cerebellar peduncles	0 (0% [0–28.4%])	1 (2% [0–11%])	>0.999
Other	0 (0% [0–28.4%])	2 (4.2% [0.6–14.2%])	>0.999
Normal MRI	0 (0% [0–28.4%])	15 (31.2% [18.6–46.2%])	0.504
Cerebrospinal fluid‡			
Positive RT-PCR SARS-CoV-2	0 (0% [0–41%])	3 (10.4% [2.2–27.4%])	>0.999
High white blood cell count	1 (14.2% [0.4–57.8%])	2 (6.8% [0.8–22.8%])	>0.999
High proteinorachia	3 (37.6% [8.6–75.6%])	8 (25% [11.4–43.4%])	>0.999
Low glycorrhachia	1 (12.4% [0.4–52.6%])	0 (0% [0–11.2%])	0.887
Elevated Immunoglobulin G	2 (40% [5.2–85.4%])	9 (37.6% [18.8–59.4%])	>0.999
Presence of oligoclonal IgG bands	1 (20% [0.6–71.6%])	6 (25% [9.8–46.8%])	>0.999

† Uncorrected confidence intervals, p-values corrected for multiple testing with a 5% false discovery rate.
‡ Data not available for all patients.

MRI delays and abnormal cerebral perfusion might suggest that cerebral perfusion anomalies occur in the first weeks of the disease and that brain perfusion later normalize.

The mechanisms underlying brain hypoperfusion in severe COVID-19 is uncertain. Proof of direct viral CNS infection are scarce,[19,20] and the low number of positive RT-PCR on CSF in our cohort does not support this mechanism. Rare cases of small-vessel vasculitis related to COVID-19 have been described, mostly with cutaneous and renal manifestations[21,22] but CNS lesions have also been suspected,[23] and this mechanism could explain some cases of hypoperfusion.

Hyperperfusion has been previously described in infectious leptomeningitis,[9] which probably arise from dilation of subarachnoid vessel that has long been described with arteriography in such cases.[25] As hyperperfusion in our cohort was associated with leptomeningeal enhancement, this suggests that the visually detectable parieto-temporal hyperperfusion is not specific for COVID-19 but results from meningeal hyperperfusion. The mechanism of clusters of hyperperfusion in motor cortex is less clear, but may be related to hypoxia: brain lesions (especially hemorrhage) in severe cases of COVID-19 seems frequently related to hypoxia,[11,19] and hypoxia induces an increase in CBF to (try to) maintain oxygen delivery to the brain, which can be detected with ASL perfusion.[26]

Could perfusion abnormalities be related to other factors than COVID-19?

Decreased cerebral perfusion (most often global) has been described during sedation[27,28] but no significant association with sedation was found in our cohort. Hyperoxia has been shown to reduce CBF measured with ASL[29,30] (even if the underlying mechanism is unclear between true CBF reduction or measurement errors induced by blood T1 reduction[31,32]) and may play a role in brain hypoperfusion in COVID-19 as several patients had oxygen therapy and supraphysiological PaO_2 levels. However, CBF reduction usually reported during hyperoxia appears to be more global than the regional hypoperfusion shown in patients with COVID-19.[30] Moreover, oxygen therapy in patients with COVID-19 is

Table 4
Relationship between cerebral hyperperfusion and clinical, biological and morphological parameters.

	No hyperperfusion† (*N* = 50)	Hyperperfusion† (*N* = 9)	Corrected p-value†
Men	39 (78% [64–88.4%])	5 (55.6% [21.2–86.4%])	0.887
Oxygen therapy	48 (96% [86.2–99.6%])	9 (100% [66.4–100%])	>0.999
Acute respiratory distress syndrome	43 (86% [73.2–94.2%])	8 (88.8% [51.8–99.8%])	>0.999
Hospitalized in intensive care unit at time of MRI	34 (68% [53.4–80.4%])	9 (100% [66.4–100%])	0.772
Sedation during MRI or up to 24 h **before MRI**	19 (38% [24.6–52.8%])	6 (66.6% [30–92.6%])	0.845
Death up to 30 days after MRI	5 (10% [3.4–21.8%])	1 (11.2% [0.2–48.2%])	>0.999
Chest CT findings suggestive of COVID-19‡	44 (91.6% [80–97.6%])	6 (100% [54–100%])	>0.999
Medical history			
History of stroke	6 (12% [4.6–24.4%])	1 (11.2% [0.2–48.2%])	>0.999
History of seizures	3 (6% [1.2–16.6%])	0 (0% [0–33.6%])	>0.999
Other neurological history	8 (16% [7.2–29.2%])	0 (0% [0–−33.6%])	0.962
History of hematological malignancies	2 (4% [0.4–13.8%])	1 (11.2% [0.2–48.2%])	>0.999
History of autoimmune diseases	3 (6% [1.2–16.6%])	1 (11.2% [0.2–48.2%])	>0.999
Symptoms			
Agitation	17 (34% [21.2–48.8%])	4 (44.4% [13.6–78.8%])	>0.999
Ageusia	7 (14% [5.8–26.8%])	0 (0% [0–33.6%])	>0.999
Anosmia	7 (14% [5.8–26.8%])	0 (0% [0–33.6%])	>0.999
Headaches	11 (22% [11.6–36%])	1 (11.2% [0.2–48.2%])	>0.999
Seizures	2 (4% [0.4–13.8%])	0 (0% [0–33.6%])	>0.999
Confusion	20 (40% [26.4–54.8%])	5 (55.6% [21.2–86.4%])	>0.999
Clinical signs of corticospinal tract involvement	13 (26% [14.6–40.4%])	3 (33.4% [7.4–70%])	>0.999
Disturbance of consciousness	32 (64% [49.2–77%])	8 (88.8% [51.8–99.8%])	0.919
Electroencephalogram‡			
Normal	4 (17.4% [5–38.8%])	0 (0% [0–41%])	>0.999
Under sedation	8 (34.8% [16.4–57.2%])	1 (14.2% [0.4–57.8%])	>0.999
Nonspecific	7 (30.4% [13.2–53%])	3 (42.8% [9.8–81.6%])	>0.999
Encephalopathy	4 (17.4% [5–38.8%])	3 (42.8% [9.8–81.6%])	0.962
Morphological MRI findings			
Ischemic stroke	5 (10% [3.4–21.8%])	1 (11.2% [0.2–48.2%])	>0.999
Leptomeningeal enhancement‡	14 (28.6% [16.6–43.2%])	9 (100% [66.4–100%])	0.002*
Mesial temporal lobe diffusion/FLAIR hyperintensity	12 (24% [13–38.2%])	1 (11.2% [0.2–48.2%])	>0.999
Non-confluent multifocal white matter diffusion/FLAIR hyperintense lesions with hemorrhage and variable enhancement	6 (12% [4.6–24.4%])	1 (11.2% [0.2–48.2%])	>0.999
Extensive and isolated white matter microhemorrhages	11 (22% [11.6–36%])	2 (22.2% [2.8–60%])	>0.999
Extensive and confluent supratentorial white matter FLAIR hyperintensities	1 (2% [0–10.6%])	0 (0% [0–33.6%])	>0.999
Non-confluent multifocal white matter diffusion/FLAIR hyperintense lesions with variable enhancement	4 (8% [2.2–19.2%])	0 (0% [0–33.6%])	>0.999
Diffusion/FLAIR hyperintense lesions involving both middle cerebellar peduncles	1 (2% [0–10.6%])	0 (0% [0–33.6%])	>0.999
Other	2 (4% [0.4–13.8%])	0 (0% [0–33.6%])	>0.999
Normal MRI	15 (30% [17.8–44.6%])	0 (0% [0–33.6%])	0.772
Cerebrospinal fluid‡			
Positive RT-PCR SARS-CoV-2	3 (10.8% [2.2–28.2%])	0 (0% [0–37%])	>0.999
High white blood cell count	2 (7.2% [0.8–23.6%])	1 (12.4% [0.4–52.6%])	>0.999
High proteinorachia	9 (28.2% [13.8–46.8%])	2 (25% [3.2–65%])	>0.999
Low glycorrhachia	0 (0% [0–10.8%])	1 (14.2% [0.4–57.8%])	0.852
Elevated Immunoglobulin G	10 (47.6% [25.8–70.2%])	1 (12.4% [0.4–52.6%])	0.810
Presence of oligoclonal IgG bands	5 (23.8% [8.2–47.2%])	2 (25% [3.2–65%])	>0.999

† Uncorrected confidence intervals, p-values corrected for multiple testing with a 5% false discovery rate.
‡ Data not available for all patients
*significant result

Table 5
Perfusions anomalies in each region of interest by cerebral hemisphere.

	Frontal lobe (*n* = 118)	Temporal pole (*n* = 117)*	Parietal lobe (*n* = 118)	Temporal lobe (*n* = 118)
Hypoperfusion	40 (33.9%)	52 (44.4%)	14 (11.9%)	11 (9.3%)
Normoperfusion	67 (56.8%)	59 (50.4%)	86 (72.9%)	91 (77.1%)
Hyperperfusion	11 (9.3%)	6 (5.1%)	18 (15.3%)	16 (13.6%)

* 1 patient with history of left temporal pole resection not assessable.

used to fight against hypoxemia and is tightly monitored (pulse oximetry, arterial blood gas test…), and long-lasting hyperoxia is unlikely to happen in such patients. Nevertheless, for safety purposes, some patients may have been exposed to transient high FiO_2 levels during MRI, as MRI-compatible monitoring devices sometimes provide unreliable values.

Age is a known confounding factor when studying cerebral perfusion, as CBF diminishes with age.[33,34] In this study, there was however no significant age difference between patients with brain hypoperfusion and patients without it. In subgroup analysis, the younger age of control subjects may have biased results towards more hypoperfusion in patients with COVID-19 on mean perfusion maps. However, quantitative analysis was adjusted for age, and suggested the existence of hypoperfusion in patients with COVID-19 independently of age difference.

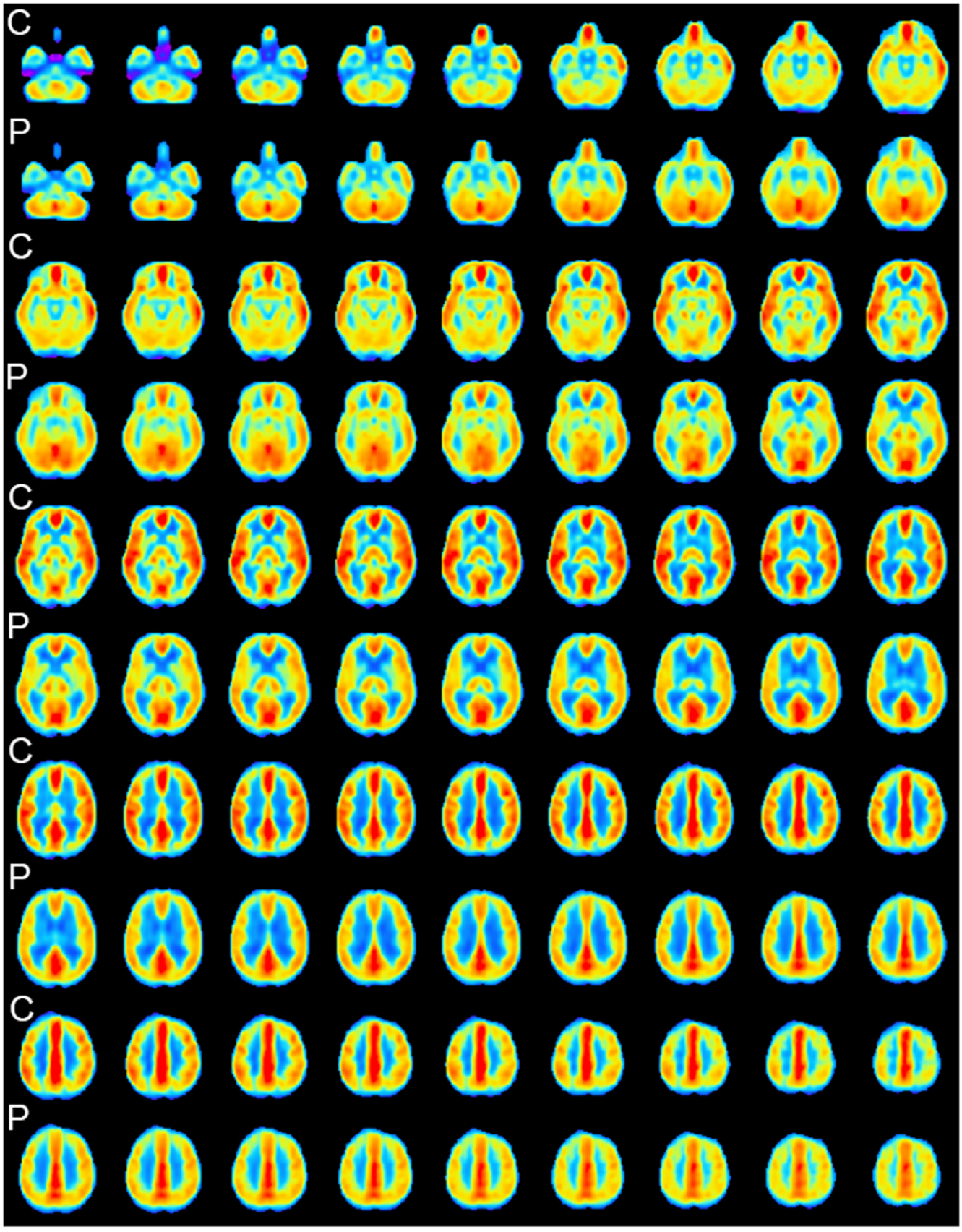

Fig. 4. Mean CBF maps of controls (C) and patients (P) in subgroup analysis.

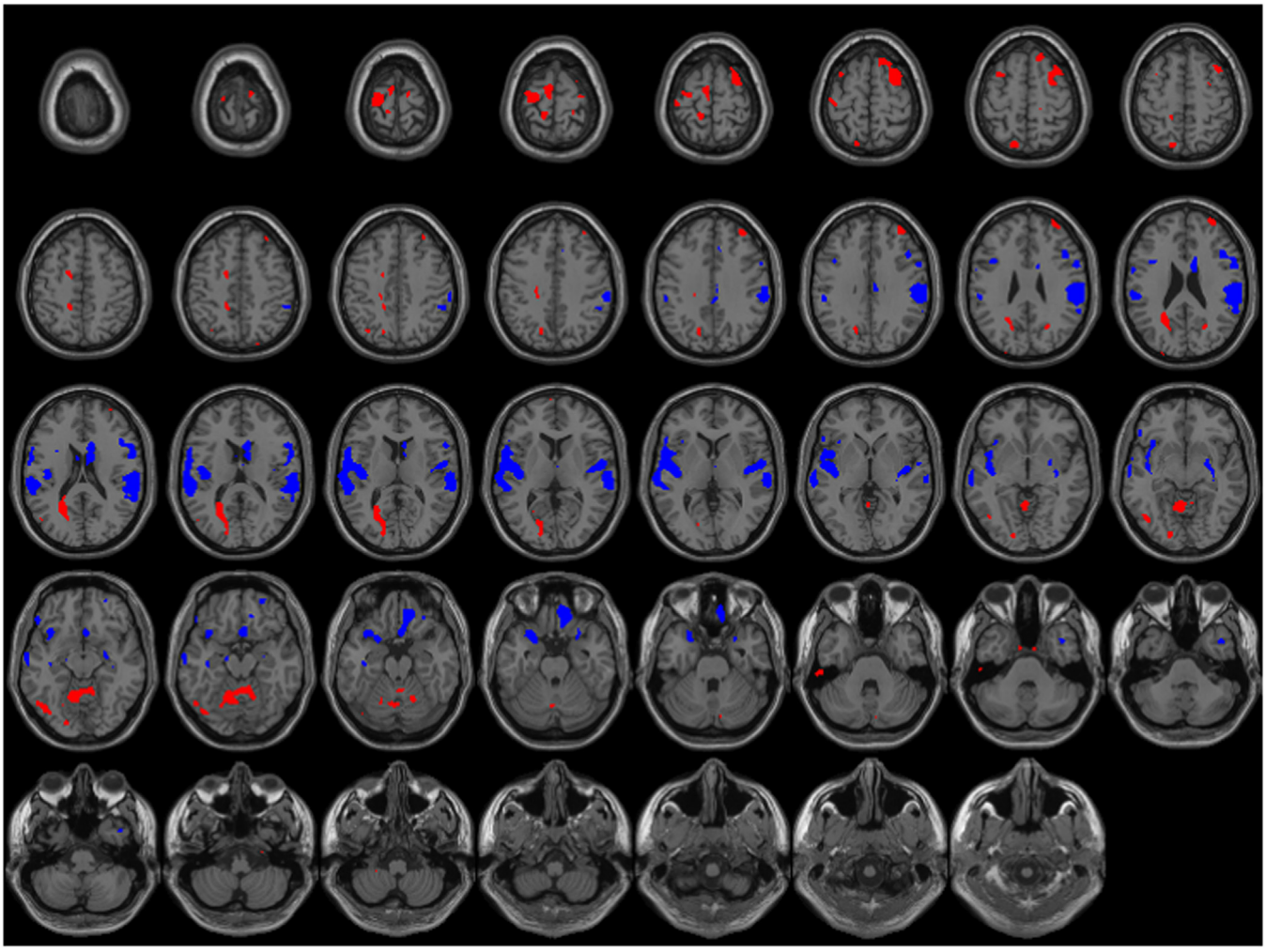

Fig. 5. Comparison of cerebral blood flow (CBF) adjusted for age and sedation from patients with COVID-19 and healthy subjects. Z-score maps thresholded with p-value $< 10^{-3}$ projected on a template brain image. Blue areas: lower CBF in patients with COVID-19. Red areas: higher CBF in patients with COVID-19.

Links between ASL perfusion and other modalities of brain exploration

EEG has been widely used to assess neurological manifestations in patients with COVID-19. Results vary across studies, as several EEG features have been analyzed. Our findings, with 57% of patients (who had an EEG) with either non-specific or encephalopathic alterations, are in accordance with previous findings.[35] Brain electrical activity is coupled with perfusion, and EEG alterations have been associated with hypoperfusion in Alzheimer's disease.[36] Interestingly, in COVID-19, EEG modifications are more frequent in the frontal regions.[37] This predominant frontal pattern may be linked to the fronto-temporal hypoperfusion that we report. We did not find a significant association between perfusion and EEG abnormalities, but this might come from the global "clinical" classification we used instead of detailed regional electrical abnormalities.

Frontal lobe hypometabolism has been described[38] with 18-fluorodeoxyglucose positron emission tomography in a 77 year old woman suffering from COVID-19 during a transient frontal encephalopathy and normal morphological MRI. Cerebral perfusion was not assessed. The metabolic pattern described by Fox et al. is however similar to the hypoperfusion pattern we are reporting, and the coupling between brain glucose metabolism and perfusion is well established.[39]

Abnormal functional findings (with ASL perfusion or with 18-fluorodeoxyglucose positron emission tomography) might be helpful to understand some symptoms exhibited by patients with severe COVID-19, especially in the absence of morphological MRI alteration. We hypothesize that focal hyperperfusion in motor cortex might have a link with signs of corticospinal tract involvement reported in some of our patients. And even if we did not find a significant relationship between psychomotor agitation and frontal hypoperfusion in this study, such a relationship has been shown in patients with fronto-temporal forms of dementia or frontal lobe syndrome who exhibit frontal hypoperfusion[40] which severity correlates with the severity of their symptoms.[41]

The short- and long-term functional outcome of patients with severe COVID-19 and brain perfusion abnormalities needs to be further investigated. However, a recently published follow-up of patients with COVID-19 and initial neurological symptoms,[42] of whom 68% had MRI abnormalities (including perfusion abnormalities), shows that nearly half of them had persistent slightly diminished results in working memory and executive functions testing. Alteration of such frontal neurocognitive functions might have a link with the fronto-temporal pattern of hypoperfusion that we report.

This study has some limitations. The most important one is that we did not have intensive care patients with other conditions as controls, to limit confounding factors like sedation. However, cerebral perfusion did not significantly differ in our study between patients admitted to intensive-care units and those admitted to other wards. This study is also at risk of bias due to its retrospective nature: for example, data on oxygen therapy and anesthetic drugs used at the time of MRI were missing. In addition, MRI from multiple centers

with different MRI scanners increased the heterogeneity of ASL data. Classification of the morphological MRI anomalies was based on previously described lesions[11] but there is presently no consensus or general guideline regarding the classification of brain MRI abnormalities in COVID-19.

Conclusion

We report cerebral perfusion anomalies in a large multicentric cohort of patients with severe COVID-19. Hypoperfusion was the most frequently encountered anomaly, occurring in frontal and temporopolar pattern. Hyperperfusion was more uncommon, mostly located in parieto-temporal regions, and linked to leptomeningeal enhancement. Mechanisms underlying hypoperfusion remains unclear, but our data suggest that sedation in ICU patients is not sufficient to explain it. ASL perfusion may be helpful to assess patients with neurological symptoms during COVID-19.

Declaration of Competing Interest

The authors declare that they have no known competing financial interests or personal relationships that could have appeared to influence the work reported in this paper.

Acknowledgment

The authors want to thank Pr. Marie-Cécile Henry-Feugeas for participating in the collection of brain MRI of patients with COVID-19 and for sharing these data.

References

1. Dong E, Du H, Gardner L. An interactive web-based dashboard to track COVID-19 in real time. *Lancet Infect Dis*. 2020;20:533–534. https://doi.org/10.1016/S1473-3099(20)30120-1.
2. Gandhi RT, Lynch JB, del Rio C. Mild or Moderate Covid-19. *N Engl J Med*. 2020;383:1757–1766. https://doi.org/10.1056/NEJMcp2009249.
3. Mao L, Jin H, Wang M, et al. Neurologic manifestations of hospitalized patients with coronavirus disease 2019 in Wuhan, China. *JAMA Neurol*. 2020;77:683. https://doi.org/10.1001/jamaneurol.2020.1127.
4. Helms J, Kremer S, Merdji H, et al. Neurologic features in severe SARS-CoV-2 infection. *N Engl J Med*. 2020;382:2268–2270. https://doi.org/10.1056/NEJMc2008597.
5. Paterson RW, Brown RL, Benjamin L, et al. The emerging spectrum of COVID-19 neurology: clinical, radiological and laboratory findings. *Brain*. 2020;143:3104–3120. https://doi.org/10.1093/brain/awaa240.
6. Kremer S, Lersy F, Anheim M, et al. Neurologic and neuroimaging findings in patients with COVID-19: a retrospective multicenter study. *Neurology*. 2020;95:e1868–e1882. https://doi.org/10.1212/WNL.0000000000010112.
7. Chougar L, Shor N, Weiss N, et al. Retrospective observational study of brain MRI findings in patients with acute SARS-CoV-2 infection and neurologic manifestations. *Radiology*. 2020;297:E313–E323. https://doi.org/10.1148/radiol.2020202422.
8. Alsaedi A, Thomas D, Bisdas S, Golay X. Overview and critical appraisal of arterial spin labelling technique in brain perfusion imaging. *Contrast Media Mol Imaging*. 2018;2018:1–15. https://doi.org/10.1155/2018/5360375.
9. Noguchi T, Yakushiji Y, Nishihara M, et al. Arterial spin-labeling in central nervous system infection. *Magn Reson Med Sci*. 2016;15:386–394. https://doi.org/10.2463/mrms.mp.2015-0140.
10. Vallabhaneni D, Naveed MA, Mangla R, et al. Perfusion imaging in autoimmune encephalitis. *Case Rep Radiol*. 2018;2018:1–4. https://doi.org/10.1155/2018/3538645.
11. Kremer S, Lersy F, de Sèze J, et al. Brain MRI findings in severe COVID-19: a retrospective observational study. *Radiology*. 2020;297:E242–E251. https://doi.org/10.1148/radiol.2020202222.
12. R Core Team. *R: A language and environment for statistical computing*. Vienna, Austria: R Foundation for Statistical Computing; 2020. https://www.R-project.org/.
13. Launes J, Lindroth L, Liewendahl K, et al. Diagnosis of acute herpes simplex encephalitis by brain perfusion single photon emission computed tomography. *Lancet N Am Ed*. 1988;331:1188–1191. https://doi.org/10.1016/S0140-6736(88)92010-7.
14. Barai S, Sanjay G, Shankar PD, Manish O. Sequential brain perfusion abnormalities in various stages of Japanese encephalitis. *Hell J Nucl Med*. 2006;9:163–166.
15. Tyrakowska-Dadełło Z, Tarasów E, Janusek D, et al. Brain perfusion alterations in tick-borne encephalitis—preliminary report. *Int J Infect Dis*. 2018;68:26–30. https://doi.org/10.1016/j.ijid.2018.01.002.
16. Mungunkhuyag M, Harada M, Abe T, et al. Longitudinal monitoring with multiple MR techniques in a case of progressive multifocal leukoencephalopathy associated with multiple myeloma. *Magn Reson Med Sci*. 2014;13:55–59. https://doi.org/10.2463/mrms.2013-0037.
17. Chang L, Shukla DK. Imaging studies of the HIV-infected brain. In:. *Handbook of Clinical Neurology*. Elsevier; 2018:229–264.
18. Lapucci C, Boffa G, Massa F, et al. Could arterial spin labelling perfusion imaging uncover the invisible in N-methyl-D-aspartate receptor encephalitis? *Eur J Neurol*. 2019;26:e86–e87. https://doi.org/10.1111/ene.13977.
19. Solomon IH, Normandin E, Bhattacharyya S, et al. Neuropathological features of COVID-19. *N Engl J Med*. 2020;383:989–992. https://doi.org/10.1056/NEJMc2019373.
20. Rhea EM, Logsdon AF, Hansen KM, et al. The S1 protein of SARS-CoV-2 crosses the blood–brain barrier in mice. *Nat Neurosci*. 2021;24:368–378. https://doi.org/10.1038/s41593-020-00771-8.
21. Colonna C, Monzani NA, Rocchi A, et al. Chilblain-like lesions in children following suspected COVID-19 infection. *Pediatr Dermatol*. 2020;37:437–440. https://doi.org/10.1111/pde.14210.
22. Berteloot L, Berthaud R, Temmam S, et al. Arterial abnormalities identified in kidneys transplanted into children during the COVID-19 pandemic. *Am J Transplant*. 2021;16464. https://doi.org/10.1111/ajt.16464. ajt.
23. Hanafi R, Roger P-A, Perin B, et al. COVID-19 neurologic complication with CNS vasculitis-like pattern. *Am J Neuroradiol*. 2020;41:1384–1387. https://doi.org/10.3174/ajnr.A6651.
24. Ferris EJ, Rudikoff JC, Shapiro JH. Cerebral angiography of bacterial infection. *Radiology*. 1968;90:727–734. https://doi.org/10.1148/90.4.727.
25. Harris AD, Murphy K, Diaz CM, et al. Cerebral blood flow response to acute hypoxic hypoxia. *NMR Biomed*. 2013;26:1844–1852. https://doi.org/10.1002/nbm.3026.
26. Liang P, Xu Y, Lan F, et al. Decreased cerebral blood flow in mesial thalamus and precuneus/PCC during midazolam induced sedation assessed with ASL. *Neuroinformatics*. 2018;16:403–410. https://doi.org/10.1007/s12021-018-9368-y.
27. Kaisti KK, Metsähonkala L, Teräs M, et al. Effects of surgical levels of propofol and sevoflurane anesthesia on cerebral blood flow in healthy subjects studied with positron emission tomography. *Anesthesiol J Am Soc Anesthesiol*. 2002;96:1358–1370.
28. Floyd TF, Clark JM, Gelfand R, et al. Independent cerebral vasoconstrictive effects of hyperoxia and accompanying arterial hypocapnia at 1 ATA. *J Appl Physiol*. 2003;95:9. https://doi.org/10.1152/japplphysiol.00303.2003.
29. Bulte DP, Chiarelli PA, Wise RG, Jezzard P. Cerebral perfusion response to hyperoxia. *J Cereb Blood Flow Metab*. 2007;27:69–75. https://doi.org/10.1038/sj.jcbfm.9600319.
30. Pilkinton DT, Hiraki T, Detre JA, et al. Absolute cerebral blood flow quantification with pulsed arterial spin labeling during hyperoxia corrected with the simultaneous measurement of the longitudinal relaxation time of arterial blood. *Magn Reson Med*. 2012;67:1556–1565. https://doi.org/10.1002/mrm.23137.
31. Siero JCW, Strother MK, Faraco CC, et al. *In vivo* quantification of hyperoxic arterial blood water T1. *NMR Biomed*. 2015;28:1518–1525. https://doi.org/10.1002/nbm.3411.
32. Liu Y, Zhu X, Feinberg D, et al. Arterial spin labeling MRI study of age and gender effects on brain perfusion hemodynamics. *Magn Reson Med*. 2012;68:912–922. https://doi.org/10.1002/mrm.23286.
33. Zhang N, Gordon ML, Goldberg TE. Cerebral blood flow measured by arterial spin labeling MRI at resting state in normal aging and Alzheimer's disease. *Neurosci Biobehav Rev*. 2017;72:168–175. https://doi.org/10.1016/j.neubiorev.2016.11.023.
34. Petrescu A-M, Taussig D, Bouilleret V. Electroencephalogram (EEG) in COVID-19: a systematic retrospective study. *Neurophysiol Clin*. 2020;50:155–165. https://doi.org/10.1016/j.neucli.2020.06.001.
35. Moretti DV. Electroencephalography reveals lower regional blood perfusion and atrophy of the temporoparietal network associated with memory deficits and hippocampal volume reduction in mild cognitive impairment due to Alzheimer's disease. *Neuropsychiatr Dis Treat*. 2015;11:461–470. https://doi.org/10.2147/NDT.S78830.
36. Antony AR, Haneef Z. Systematic review of EEG findings in 617 patients diagnosed with COVID-19. *Seizure*. 2020;83:234–241. https://doi.org/10.1016/j.seizure.2020.10.014.
37. Cani I, Barone V, D'Angelo R, et al. Frontal encephalopathy related to hyperinflammation in COVID-19. *J Neurol*. 2021;268:16–19. https://doi.org/10.1007/s00415-020-10057-5.
38. Fox PT, Raichle ME, Mintun MA, Dence C. Nonoxidative glucose consumption during focal physiologic neural activity. *Science*. 1988;241:462–464. https://doi.org/10.1126/science.3260686.
39. Rohrer JD, Rosen HJ. Neuroimaging in frontotemporal dementia. *Int Rev Psychiatry*. 2013;25:221–229. https://doi.org/10.3109/09540261.2013.778822.
40. Maiovis P, Ioannidis P, Gerasimou G, et al. frontotemporal lobar degeneration-modified clinical dementia rating (FTLD-CDR) scale and frontotemporal dementia rating scale (FRS) correlation with regional brain perfusion in a series of FTLD patients. *J Neuropsychiatry Clin Neurosci*. 2016;29:26–30. https://doi.org/10.1176/appi.neuropsych.16020034.
41. Lersy F, Bund C, Anheim M, et al. Evolution of neuroimaging findings in severe COVID-19 patients with initial neurological impairment: an observational study. *Viruses*. 2022;14:949. https://doi.org/10.3390/v14050949.